THE ASTROPHYSICAL JOURNAL, 544:L7–L10, 2000 November 20

PROBING THE WARM INTERGALACTIC MEDIUM THROUGH ABSORPTION AGAINST GAMMA-RAY BURST X-RAY AFTERGLOWS

F. FIORE,[1] F. NICASTRO,[1,2] S. SAVAGLIO,[1] L. STELLA,[1] AND M. VIETRI[3]
Received 2000 June 16; accepted 2000 September 15; 2000 November 1

ABSTRACT

Gamma-ray burst (GRB) afterglows close to their peak intensity are among the brightest X-ray sources in the sky. Despite their fast power-law–like decay, when fluxes are integrated from minutes up to hours after the GRB event, the corresponding number counts ($\log N$–$\log F$ relation) far exceed those of any other high-redshift ($z > 0.5$) source, the flux of which is integrated over the same time interval. We discuss how to use X-ray afterglows of GRBs as distant beacons to probe the warm (10^5 K $< T < 10^7$ K) intergalactic matter in filaments and outskirts of clusters of galaxies by means of absorption features, the "X-ray forest." According to current cosmological scenarios, this matter may comprise 30%–40% of the baryons in the universe at $z < 1$. Present-generation X-ray spectrometers such as those on *Chandra* and *XMM-Newton* can detect it along most GRBs' lines of sight, provided afterglows are observed soon enough (within hours) after the burst. A dedicated medium-sized X-ray telescope (effective area $\lesssim 0.1$ m^2) with pointing capabilities similar to that of *Swift* (minutes) and high spectral resolution ($E/\Delta E \gtrsim 300$) would be very well suited to exploit the new diagnostic and study the physical conditions in the universe at the critical moment when structure is being formed.

Subject headings: cosmology: observations — gamma rays: bursts — large-scale structure of universe

1. INTRODUCTION

Gamma-ray burst (GRB) afterglows carry a relatively large fraction of the total GRB flux, often exceeding the total energy budget of the main event itself. Minutes after the GRB events, they are by far the brightest sources in the sky at cosmological redshifts (nine GRB redshifts have been measured so far, ranging between $z = 0.4$ and $z = 3.4$ with a median of about $z = 1.3$). For this reason the optical and infrared GRB afterglows have been proposed as probes of the high-redshift universe through the detection of absorption-line systems along the line of sight (Lamb & Reichart 2000; Ciardi & Loeb 2000). However, optical and infrared afterglows have been detected in less than half of the GRBs observed by *BeppoSAX*. Moreover, they carry only a small fraction of the total GRB afterglow flux, most of which is in the X-ray band. We propose here to exploit X-ray resonant-scattering lines in the GRB afterglow X-ray spectra to probe the warm component of the intergalactic medium (IGM).

Hydrodynamic simulations show that at $z < 1$ a large fraction (30%–40%) of the baryons in the universe are in a warm phase, shock-heated to temperatures of 10^5–10^7 K during the collapse of density perturbations (see Davé et al. 2000 and references therein). According to the same simulations, 10%–20% of the remaining baryons end up in clusters of galaxies (with $T > 10^7$ K; hot phase) and 30%–40% are in stars and colder gas clouds ($T < 10^5$ K; cold phase). Both the hot and the cold phases of the IGM have been detected and studied in detail in the X-ray and O UV bands, respectively. The cold gas is revealed through UV rest-frame absorption lines. At $z > 1.5$ these lines are redshifted in the optical and are thus easily detected in the spectra of bright background sources such as quasars. At $z \lesssim 1.5$, their study is complicated by the limited capabilities of UV instruments. Hot gas shines in the 0.1–10 keV band as a result of bremsstrahlung emission and line emission, both proportional to the square of the gas density and so primarily tracing peak densities. On the other hand, observations of the warm IGM expected away from the high-density regions have yielded so far only limited information. Gas with $T \approx 10^5$ K has been revealed through O VI absorption at 1032 and 1038 Å at $z = 0.1$–0.3 (Tripp, Savage, & Jenkins 2000; Tripp & Savage 2000). O VI has been detected at $z = 2$–4 also (Kirkman & Tytler 1997, 1999), but in these cases the O VI lines are probably associated with Lyman limit systems [$16 < \log N(\mathrm{H\ I}) < 19$] and therefore with colder gas clouds in galaxies. Warmer IGM (10^6 K $< T < 10^7$ K) can be detected and studied by measuring both the photoelectric absorption edges and the resonant-scattering lines of C, O, Ne, Si, S, Mg, Fe, etc., in the X-ray spectra of bright background objects (the X-ray Gunn-Peterson test; Sherman & Silk 1979; Shapiro & Bahcall 1980; Aldcroft et al. 1994; Markevitch 1999). X-ray spectroscopy of absorption edges and resonant-scattering lines is the *only* tool to probe such a warm, low-density gas. In fact, the strength of these features is linearly proportional to the gas density, and therefore, below a critical value absorption wins over emission. This can be seen best by studying with adequate energy resolution ($E/\Delta E \gtrsim 300$) a bright background source. Previous studies proposed quasars as background objects (Aldcroft et al. 1994; Hellsten, Gnedin, & Miralda-Escudé 1998; Perna & Loeb 1998b). The problem is that X-ray bright $z \gtrsim 0.3$ quasars are rare: only nine of the 96 AGNs in the *HEAO 1* Grossan (1992) sample (flux of $S_{2-10\ \mathrm{keV}} \gtrsim 1.5 \times 10^{-11}$ ergs cm^{-2} s^{-1}) have $z > 0.3$ and only three have $z > 1$. Only these AGNs can provide a few times 10^4 counts in deep (≈100 ks) exposures with present-generation X-ray satellites (*Chandra* and *XMM-Newton*). The systematic study of the warm IGM using fainter AGNs must then await missions of the size of *Constellation-X*[4] and *XEUS*[5] (collecting area of 1–10 m^2) foreseen for the next decade. We find instead that *every* GRB X-ray afterglow can provide enough counts to

[1] Osservatorio Astronomico di Roma, Via Frascati 33, I-00044 Monteporzio Catone, Italy.
[2] Harvard-Smithsonian Center for Astrophysics, 60 Garden Street, Cambridge, MA 02138.
[3] Dipartimento di Fisica, Università Roma Tre, via della Vasca Navale 84, I-00146 Roma, Italy.

[4] See, e.g., http://constellation.gsfc.nasa.gov/science/igm2.html.
[5] See ftp://astro.estec.esa.nl/pub/XEUS/BROCHURE/brochure.ps.gz and http://www.ias.rm.cnr.it/sax/probing.html.

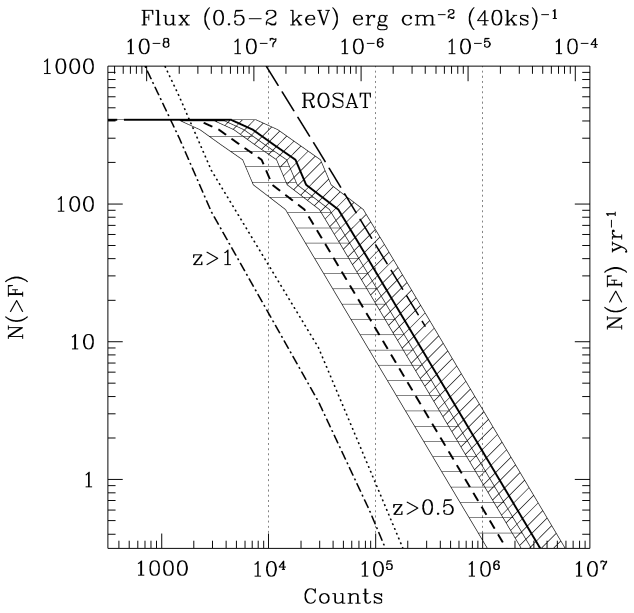

FIG. 1.—Number of GRBs at high Galactic latitude vs. 0.5–2 keV fluence, i.e., the flux integrated in 40 ks (*upper x-axis*), and the corresponding counts accumulated in 40 ks by an instrument with the throughput of the *XMM* RGS (one unit; *lower x-axis*). Fast GRBs (duration of $\lesssim$3 s) contribute to $\sim$30% of the total. An intrinsic GRB $N_{\rm H}$ of 10^{21} cm^{-2} (*thick solid line*) and 3×10^{21} cm^{-2} (*thick-dashed line*) as seen at redshift $\lesssim$0.3 is assumed. These lines are computed for a power-law GRB decay index of $\delta = -1.3$. The shaded bands surrounding each thick line have $\delta = -1.1$ as the right-hand boundary and $\delta = -1.5$ as the left-hand boundary. The long-dashed line is the *ROSAT* log N–log F. The dotted line and the dot-dashed line show the log N–log F of the $z > 0.5$ and $z > 1$ *ROSAT* sources, respectively. Vertical dotted lines mark spectra with 10^4, 10^5, and 10^6 counts, respectively.

study the warm IGM by using medium-high resolution X-ray spectroscopy if observed within a few minutes after the GRB event. In just 1 yr of activity, an instrument with the effective area of an *XMM-Newton* or *Astro-E* mirror unit and a high-resolution focal plane detector (such as a grating or a calorimeter) may study accurately tens to hundreds of lines of sight. The study of the warm filaments and cluster outskirts, possibly complemented with UV absorption studies, will provide new crucial information on the phase at which galaxies, groups, and clusters formed, the metal enrichment and heating histories of the IGM, and the feedback between hot and warm halos and star formation in galaxies (see, e.g., Cavaliere, Giacconi, & Menci 2000).

2. THE X-RAY log N–log F OF GRBs AND OTHER HIGH-z SOURCES

The study of afterglows starting immediately after the GRB event is the main goal of missions such as *Swift*.[6] Briefly, once a GRB is detected, the satellite is automatically maneuvered to begin imaging, within tens of seconds, the GRB region with optical and X-ray telescopes. We derive in this section the expected high Galactic latitude number counts [log N–log $F_{40}(t)$] of the X-ray afterglows as a function of the flux integrated starting from 40 s after the GRB peak up to a time t [the afterglow fluence $F_{40}(t)$]. We focus on the soft X-ray band since the main absorption features imprinted by the IGM on the GRB X-ray spectra are below $\sim$1 keV (see below).

Frontera et al. (2000a, 2000b) studied the evolution of the gamma-ray and X-ray spectra of eight GRBs seen by *BeppoSAX*. Using their spectra and light curves, we computed the ratio between the 2–10 keV flux 30–40 s after the GRB peak and the 50–300 keV flux at the peak. All points but one are in the range 0.02–0.2. The outlier, GRB 980329, has a ratio 10 times smaller and is the only GRB in the Frontera et al. (2000a) sample to show significant absorption in the 2–20 keV spectrum (see below). In the following estimates we conservatively assume a ratio of 0.01.

GRB X-ray afterglows decay with time as power laws with index δ in the range from -1 to -1.5 (Costa 1999). Substantial evidence supports the view that the X-ray afterglow starts well within the GRB duration, when the GRB spectrum softens markedly. Indeed, when the power-law decay of the X-ray afterglow observed hours to days after several GRBs is extrapolated backward in time, a good match is found with the *BeppoSAX* WFC flux a few tens of seconds after burst onset (Piro 2000; Frontera et al. 2000b). We are thus justified in estimating the fluence of the X-ray afterglow by integrating the X-ray emission starting 40 s after the GRB peak. We adopt a total integration time of 40 ks, assuming that up to this time after the main event the high-frequency cutoff of the synchrotron spectrum has not yet moved into the X-ray band. This is consistent with the fact that $\approx$90% of the bursts do display an X-ray afterglow (the few nondetections may be due to an insufficient sensitivity and/or too long a delay in the *BeppoSAX* Narrow-Field Instrument followups). The X-ray spectrum deduced from both the WFC data, acquired seconds to minutes after the burst, and the Low-Energy Concentrator-Spectrometer and the Medium-Energy Concentrator-Spectrometer spectra, acquired several hours after the burst, are consistent with a power-law model with energy index $\alpha_E \approx 1.0$. So far, there is evidence for intrinsic X-ray absorption in one GRB only: GRB 980329, $N_{\rm H} \approx 10^{22}$ cm^{-2}, assuming solar abundances (Frontera et al. 2000a; Owens et al. 1998). All other GRBs analyzed by Owens et al. (1998) have a measured column density at the GRB redshift, where available, consistent with 0 at the 2 σ level. Excluding the GRB 980329 event, the average best-fit $N_{\rm H}$ at the GRB redshifts is 2.5×10^{21} cm^{-2}. Since the column density computed in the observer frame scales roughly as $(1 + z)^{-8/3}$, the spectrum seen by a $z = 0.1$–0.3 IGM cloud has an effective cutoff corresponding to an $N_{\rm H} \approx 0.5$ times that obtained at the mean GRB redshift of 1. We conservatively assume in the following a GRB $N_{\rm H}$ in the range (1–3) $\times$ 10^{21} cm^{-2} *as seen by a gas cloud at* $z \lesssim 0.3$.

The GRB peak flux log N–log S relationship is well known from 10^{-8} to 10^{-4} ergs cm^{-2} s^{-1} (50–300 keV; see, e.g., Fishman & Meegan 1995). Using the relationship between the GRB peak flux and the 2–10 keV emission 30–40 s after the peak and assuming the X-ray spectral shape discussed above, we predict the log N–log S of the 0.5–2 keV X-ray emission as it will be first seen by satellites with reaction capabilities similar to those of *Swift*. Figure 1 shows the number of objects at high Galactic latitude (i.e., in half of the sky) as a function of the 0.5–2 keV flux integrated in 40 ks (the fluence F, *upper scale*) and of the total counts accumulated in 40 ks by an instrument with the effective area of the *XMM-Newton* Reflection Grating Spectrometer (RGS; one unit). The GRB log N–log F is compared to the *ROSAT* log N–log F (adapted from Hasinger et al. 1998). This is dominated at high fluxes by *nearby* Seyfert galaxies and BL Lacertae objects. Most of the IGM is beyond the brightest 0.5–2 keV sources in the sky. The dotted line and the dot-dashed line show the number of 0.5–2 keV sources with $z > 0.5$ and $z > 1$, respectively, as estimated using the soft X-ray log N–log S of bright blazars (e.g., Wolter et al. 1991), the fraction of identified AGNs in the *ROSAT* all-sky survey,

[6] *Swift* will be launched in 2003; see http://swift.sonoma.edu.

TABLE 1
EQUIVALENT WIDTH OF THE STRONGEST RESONANT LINES

T (K)	C V (eV)	C VI (eV)	O VII (eV)	O VIII (eV)	Ne (eV)	Fe (eV)
$10^{5.5}$	0.63–0.36	...	1.12–0.55	...	...	...
$10^{6.0}$	0.42–0.16	0.23–0.37	1.16–0.72	...	0.65–0.17[a]	0.11[b]
$10^{6.5}$	...	0.01–0.02	0.43–0.12	0.31–0.53	0.56–0.14[a]	0.31[c]
$10^{7.0}$	...	...	...	0.02–0.04	0.04[d]	0.10[e]

NOTE.—Kα and Kβ line EWs are reported for the C, O, and Ne ions.
[a] Ne IX line.
[b] Fe IX line.
[c] Fe XVII line.
[d] Ne X line.
[e] Fe XX line.

and the results of synthetic AGN models for the X-ray background (Comastri et al. 1995). Figure 1 shows that under our conservative assumption there should be a few lines of sight per month with $\gtrsim 10^5$ counts. A few lines of sight per year may be studied with more than 10^6 counts. These estimates have to be compared with ≈10 lines of sight in total that can be studied with $\gtrsim 10^5$ counts by using $z > 0.5$ AGNs as background beacons. We remark that this result strongly depends on the speed with which the afterglow is observed, i.e., for $\delta = -1.3$, twice as many photons are emitted between t_0 and $10t_0$ than are emitted between $10t_0$ and $100t_0$.

3. X-RAY ABSORPTION FEATURES FROM THE IGM

In order to study the warm IGM with background beacons, metal abundances must be sufficiently high that relatively strong absorption features are produced. Using numerical simulations, Cen & Ostriker (1999) estimate a metallicity of at least 0.1 $Z_\odot$ for $z < 0.5$, depending on the gas density. This is supported by several pieces of evidence. First, the metallicity of the hot intracluster medium is found to be ≈0.3 $Z_\odot$ in many cases. Second, collisionally excited O VI lines have been detected at $z < 0.3$ (Tripp et al. 2000; Tripp & Savage 2000). Third, C IV and Si IV associated with Lyα clouds have been detected at $z > 1.5$ (e.g., Songaila & Cowie 1996; Ellison et al. 1999) Finally, the nine damped Lyα systems with detected metals and $z < 0.7$ have a metallicity in the range 0.4–0.6 $Z_\odot$ (Savaglio, Panagia, & Stiavelli 1999), indicating that galaxies at $z < 0.7$ can provide metals to the IGM.

The IGM transmitted spectrum can be used as a diagnostic of temperature, metal abundances, column and volume densities, and gasdynamics. We calculated the line strength and profiles expected from a cloud of gas at a given redshift, with given temperature, column density, and metal abundance using the code of Nicastro, Fiore, & Matt (1999a). Ionization equilibrium was calculated using CLOUDY (Ferland 1999). Table 1 gives the equivalent width (EW) of the strongest resonant lines in four simulations for a cloud at $z = 0.1$ and of equivalent hydrogen column density of $N_{\rm H} = 10^{20}$ cm^{-2}, metal abundance of 0.3 $Z_\odot$, $b = 200$ km s^{-1} (the Doppler term b includes also gas turbulence), and temperatures $T = 10^{5.5}$, 10^6, $10^{6.5}$, and 10^7 K. Kα and Kβ resonant transitions from He- and H-line ions of C, O, and Ne produce the strongest features in the 0.2–3 keV band, along with a series of L resonant lines from Mg, S, Si, and Fe. At $T = 10^{5.5}$ K, C V and O VII are the dominant ions (their relative abundance being >80%). At $T = 10^6$ K, He-like ions of C, O, and Ne are still dominant, but H-like C is visible. At $T = 10^{6.5}$ K, O VIII is the dominant oxygen ion. A relatively strong Fe XVII line at 0.825 keV is also visible. For $T = 10^7$ K, oxygen is nearly completely ionized, and only a weak L "forest" from highly ionized iron is present in the spectrum around 1 keV (Fe XX at 0.967 keV being the strongest line). Reducing b by a factor of 2 will reduce the EW by ≈30%. Figure 2 shows how the spectra with $T = 10^6$ K and $T = 10^{6.5}$ K would be measured by a typical grating (resolution of ~1000 at 0.3 eV, 500 at 0.5 keV, and ~300 at 0.8 keV, and with similar sensitivity in this band). We assumed 10^5 counts (0.5–2 keV) in each spectrum. With this signal-to-noise ratio (~10 eV^{-1}) and with a resolution of 1 eV at 0.5 keV, O VII and O VIII lines of EW = 0.5–1 eV can be easily detected. In fact, the minimum EW detectable with a signal-to-noise ratio of 5 given the above constraints is ~0.5 eV (using eq. [12] of Perna & Loeb 1998b). Ne and Fe lines of similar EW are more difficult to detect as a result of the reduced resolution at increasing energies. Interestingly, C V and C VI lines at 0.3–0.4 keV of EW of only 0.3–0.4 eV are also easily detectable thanks to the ~0.3 eV resolution of the gratings at those energies. Our simulation shows that oxygen of column densities as low as $N_{\rm H} = (2\text{–}4) \times 10^{16}$ cm^{-2} can be detected in such high-quality spectra at $z = 0.1$. Columns smaller by a factor of ≈2 may be detected at $z \approx 1$, where the O VII and O VIII lines are redshifted to ≈0.3 keV, again as a result of the improved resolution of gratings at low energies.

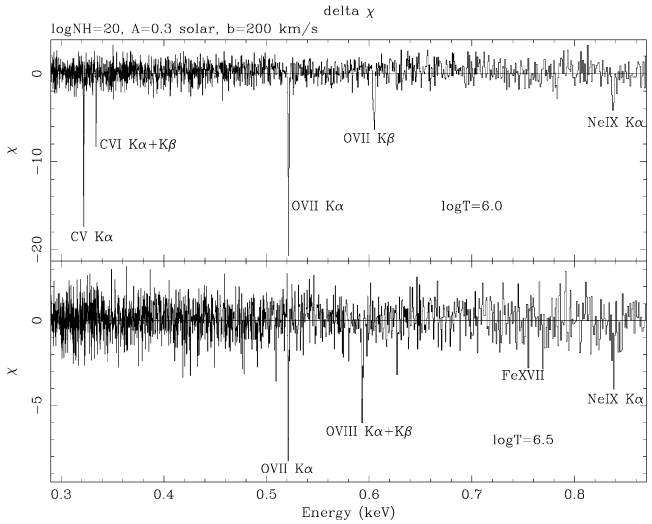

FIG. 2.—Residuals after subtraction of the best-fit continuum from simulations of grating spectra transmitted by a cloud of gas at $z = 0.1$ and of $N_{\rm H} = 10^{20}$ cm^{-2}, metal abundances 0.3 $Z_\odot$, $b = 200$ km s^{-1}, and $T = 10^6$ and $10^{6.5}$ K. See the text for details.

Our calculations adopt a collisional ionization equilibrium, whereas photoionization from cosmic X-ray and UV backgrounds and from possible nearby sources such as AGNs and starburst galaxies is expected to alter the relative ionic abundances, making their distributions as a function of the temperature wider than in the collisional case (Nicastro et al. 1999b). The contribution of photoionization to the gas ionization state is increasingly important for decreasing gas densities. In this case, the measurement of the EW of at least three lines of the same element can be used as temperature *and* density diagnostics. The contribution of the afterglow itself to the gas ionization is negligible for distances higher than a few megaparsecs. The maximum number of ionizations per event is in fact $\approx 5 \times 10^{62}$, and assuming conservatively that all the gas in the IGM has $T = 10^6$ K and that the mean density is 5×10^{-7} cm^{-3}, the radius of the ionized bubble is $\lesssim 3$ Mpc (also see Perna & Loeb 1998a).

Finally, we note that, in principle, combination of multiple absorption systems along a line of sight could complicate the resulting emerging spectrum, making the identification of the single components more difficult. O VII and O VIII Kα and Kβ lines are by far the most intense lines expected in a broad temperature range. Several authors evaluated the distribution of the oxygen line EW per unit redshift (Hellsten et al. 1998) or the probability to observe a given line EW per unit redshift (Perna & Loeb 1998b; K. Jahoda, G. Madejski, & C. Stahle 2000[7]). The results indicate that a random line of sight up to $z = 0.3$–0.5 should contain the order of one system, or a few systems at most, with O VII or O VIII of EW $\gtrsim 0.5$ eV, easing the line identification process.

4. DISCUSSION AND CONCLUSIONS

The X-ray band provides a unique opportunity to probe the warm IGM through the detection of the so-called X-ray forest. On the contrary, UV O VI lines can probe relatively low temperature plasmas only. We have shown that afterglows of GRBs can provide the most effective X-ray beacons at high z to study absorption features due to the warm IGM. A few afterglows per year should be bright enough, 2–4 hr after the main event, to produce spectra with 10,000–100,000 counts in the *Chandra* and *XMM* gratings, thus allowing the detection of warm IGM with H equivalent column density of $\gtrsim 10^{20}$ cm^{-2}. This can then be used to constrain the baryon cosmological mass density, independent of nucleosynthesis calculations. *Swift*, currently the only planned satellite with a much faster pointing capability (minutes), will allow the detection of absorption edges and blended lines from higher density regions ($N_{\rm H} \gtrsim 10^{21}$ cm^{-2}) with the resolution afforded by its CCDs. Maintaining the *Swift* default pointing position (i.e., when the satellite is not observing a GRB) close to the direction of large structures like the Aquarius Cluster concentration (Markevitch 1999), the Shapley supercluster, etc., would increase the probability of observing a GRB behind these high-density structures. This, in turn, would increase the probability of detecting the warm IGM component, if it is associated with the filaments connecting high-density regions as predicted by current cosmological scenarios (Davé et al 2000). Detection of significant absorption in these lines of sight would provide at the same time a first, direct, a priori test of the growth of large-scale structure in the universe.

More ambitiously, the technology and most of the hardware to put together a mission with the *Swift* slew capability, $\sim$0.1 m^2 collecting area and high-resolution capabilities (such those provided by gratings or calorimeters), is currently available. The *Swift* trigger might be used by such a mission to slew quickly on a GRB event. Gratings can provide enough resolution to detect oxygen lines of EW $\gtrsim 0.5$ eV at $z = 0.1$–0.3 and, most intriguingly, EW of a few tenths of an electron volt at $z \sim 1$. This will allow us to probe oxygen columns as small as 10^{16} cm^{-2} at such cosmologic redshifts. Moreover, it might be worth considering upgrading the slew capabilities of satellites such as *Constellation-X* and *XEUS*. These satellites will have the throughput to acquire high-resolution spectra with on order of millions of counts from GRB X-ray afterglows, provided that they can be observed soon enough after the GRB event (i.e., within 1 hr). This may allow one to push the study of the warm IGM to redshifts greater than 1 through the detection of Fe, Mg, Si, and S lines, opening the way to a *direct* test of hierarchical clustering models for the growth of structures.

This research has been partially supported by ASI contract ARS-99-75 and MURST grant Cofin-98-032. We thank A. Comastri, G. Ghisellini, G. Matt, C. Norman, P. Padovani, O. Pantano, L. Piro, N. White, and A. Wolter for useful discussions and an anonymous referee for suggestions that improved the presentation.

[7] See http://conxproject.gsfc.nasa.gov/fstjuneinfo.htm.

REFERENCES

Aldcroft, T., Elvis, M., McDowell, J., & Fiore, F. 1994, ApJ, 437, 584
Cavaliere, A., Giacconi, R., & Menci, N. 2000, ApJ, 528, L77
Cen, R., & Ostriker, J. P. 1999, ApJ, 519, L109
Ciardi, B., & Loeb, A. 2000, ApJ, 540, 687
Comastri, A., Setti, G., Zamorani, G., & Hasinger, G. 1995, A&A, 296, 1
Costa, E. 1999, A&AS, 138, 425
Davé, R., et al. 2000, ApJ, submitted (astro-ph/0007217)
Ellison, S. L., Lewis, G. F., Pettini, M., Chaffee, F. H., & Irwin, M. J. 1999, ApJ, 520, 456
Ferland, G. 1999, CLOUDY, version 90.04
Fishman, G. J., & Meegan, C. A. 1995, ARA&A, 33, 415
Frontera, F., et al. 2000a, ApJS, 127, 59
———. 2000b, ApJ, 540, 697
Grossan, B. A. 1992, Ph.D. thesis, MIT
Hasinger, G. 1998, Nucl. Phys. B, 69, 600
Hellsten, U., Gnedin, N. Y., & Miralda-Escudé, J. 1998, ApJ, 509, 56
Kirkman, D., & Tytler, D. 1997, ApJ, 489, L123
Kirkman, D., & Tytler, D. 1999, ApJ, 512, L5
Lamb, D. Q., & Reichart, D. E. 2000, ApJ, 536, 1
Markevitch, M. 1999, ApJ, 522, L13
Nicastro, F., Fiore, F., & Matt, G. 1999a, ApJ, 517, 108
Nicastro, F., Fiore, F., Perola, G. C., & Elvis, M. 1999b, ApJ, 512, 184
Owens, A., et al. 1998, A&A, 339, L37
Perna, R., & Loeb, A. 1998a, ApJ, 501, 467
———. 1998b, ApJ, 503, L135
Piro, L. 2000, preprint (astro-ph/0001436)
Savaglio, S., Panagia, N., & Stiavelli, M. 1999, preprint (astro-ph/9912112)
Shapiro, P. R., & Bahcall, J. N. 1980, ApJ, 241, 1
Sherman, R. D., & Silk, J. 1979, ApJ, 231, L61
Songaila, A., & Cowie, L. L. 1996, AJ, 112, 335
Tripp, T. M., & Savage, B. D. 2000, ApJ, 542, 42
Tripp, T. M., Savage, B. D., & Jenkins, E. B. 2000, ApJ, 534, L1
Wolter, A., Gioia, I. M., Maccacaro, T., Morris, S., & Stocke, J. T. 1991, ApJ, 369, 314